Influence of the level of connectivity on the members of the Octahedron and X-Octahedron families of tensegrities

Luisa Hernández [a], Manuel Alejandro Fernández-Ruiz [b,*], Luisa María Gil-Martín [c]

[a] CEE Undergraduate, University of Granada (UGR), E.T.S. Ingenieros de Caminos, Campus Universitario de Fuentenueva s/n. 18072 Granada, Spain
[b] Department of Civil, Materials and Manufacturing Engineering, University of Malaga (UMA), Escuela de Ingenierías Industriales, C/ Ortiz Ramos, s/n, Campus de Teatinos, 29071 Málaga, Spain
[c] Department of Structural Mechanics, University of Granada (UGR), Campus Universitario de Fuentenueva s/n, 18072 Granada, Spain

A B S T R A C T

Tensegrity structures based on topological patterns have been developed greatly in recent years. Tensegrities obtained from the same pattern are said to belong to a family. Two examples of tensegrity families are the Octahedron and the X-Octahedron, whose members are composed of rhombic and X-rhombic cells, respectively, which are collected in three groups. The general connectivity pattern of both families consists of three levels of connectivity. This work analyzes the influence of the reduction of the level of connectivity on the members of both families. The connection graphs corresponding to different levels of connectivity are defined based on the new concept of "twin tensegrities". Analytical computations have been performed to determine the force:length ratios that satisfy equilibrium, stability, and super-stability conditions. In addition, the mathematical sequence that follows the ratio between the force:length ratio of struts and cables of the X-Octahedron family that leads to a super-stable equilibrium configuration is presented. The new tensegrities obtained in this work also belong to the Octahedron and X-Octahedron families and could have promising engineering applications such as modular constructions.

1. Introduction

Tensegrity structures are free-standing, self-equilibrated, spatial structures composed of pre-stressed, pin-jointed compression and tension members (struts/bars and cables, respectively). Among others advantages, controllability and deployability of tensegrities structures made them very interesting for applications in scientific fields such as Civil Engineering [1,2], Mechanical Engineering [3], Robotics [4], Aerospace [5], Biology [6] and Architecture [7,8].

The first step in designing a tensegrity structure is to find a self-equilibrated configuration (known as the form-finding process). A review of form-finding methods of tensegrity structures can be found in [9]. The Force Density Method [10,11] (FDM) and the Dynamic Relaxation (DR) method [12] are the basis of most of form-finding methods [9].

The FDM is based on the concept of force:length ratio or force density q [10,11], which is defined as the ratio between the axial force and the length of each member of the tensegrity (q is positive for cables and negative for struts).

Form-finding methods can be classified into two types: numerical [13–19] and analytical methods [20–22]. Numerical methods are usually used for complex tensegrity structures with a high number of members while analytical ones are typically employed for simple tensegrities with a limited number of elements or a high symmetry. The advantage of the analytical form-finding methods of tensegrity structures is that they provide a thorough understanding of both the geometry and the internal stress state of the tensegrity. By using analytical form-finding methods based on FDM, a set of force:length ratios expressed in a symbolic form is computed for which the shape of the tensegrity structure is in equilibrium [20,23].

In order to simplify the computation in analytical form-finding methods, symmetric properties of tensegrities can be considered. A useful approach for identifying structural symmetry is proposed in [24]. In tensegrity structures that exhibit symmetry, the implementation of group representation theory enables form-finding analysis based on FDM to be simplified. This approach involves evaluating only a small number of block matrices instead of the full force density matrix, **D** [25]. For the specific case of tensegrity structures with dihedral symmetry, a

---

simple and efficient method to determine the self-equilibrated configuration of tensegrity structures was proposed in [26]. In [19], a numerical form-finding method is proposed where element grouping is used to reduce the total number of variables of the optimization problem.

The connectivity between the nodes of a tensegrity structure is an input to the form-finding problem. Tensegrity structures can be constructed based on geometric intuition supported by geometric bodies [22,27,28] or by using topological patterns [23,29,30]. Tensegrities obtained from a common topological pattern are grouped into tensegrity families [23,31,32]. The Octahedron [23,33], the X-Octahedron [32] and the Z-Octahedron [31,34] are examples of families of tensegrity structures found in the literature. Recently, it was found that, based on general topological rules, it is possible to generate an endless number of tensegrities of the Octahedron family [33]. New full and folded forms of tensegrities with a high number of nodes, cables and bars were discovered, all of them super-stable (i.e. stable for all levels of pre-stress and material properties of its members [35,36]).

The members of the Octahedron and X-Octahedron families are composed of rhombic and X-rhombic elementary cells, respectively (see Fig. 1). Due to the topology of these families, the elementary cells are grouped into three groups (referred to as "rows" in this work). Each row of elementary cells is connected to the other rows following the topology of the family. The above implies that there are three connectivity levels between these three rows of cells.

In previous works [23,31–34], tensegrities were defined using three levels of connectivity. In this work, the concept of twin tensegrities is first introduced. Two twin tensegrities are connected at different connectivity levels to create a single tensegrity. New tensegrity structures of the Octahedron and X-Octahedron families are obtained by modifying the level of connectivity. The influence of the level of connectivity on the stability of the resultant tensegrity is analytically studied. It has been proved that the constructability of some members of the Octahedron and X-Octahedron families improved with the reduction in the level of connectivity. This is very important for the engineering application of these tensegrity structures. Additionally, the general topological rule of the X-Octahedron [32] family is presented. Hence, an endless number of new super-stable tensegrity structures that belong to the X-Octahedron family are defined.

2. Analytical form-finding method for tensegrity structures and stability conditions

The equilibrium equations of a tensegrity with n nodes and m members can be formulated as [23,37]:

$$\begin{aligned} \mathbf{D} \cdot \mathbf{x} &= 0 \\ \mathbf{D} \cdot \mathbf{y} &= 0 \\ \mathbf{D} \cdot \mathbf{z} &= 0 \end{aligned} \tag{1}$$

In Eq.(1) $\mathbf{D} = \mathbf{C}^{\mathrm{T}}\mathbf{QC}$ $(\in \Re^{n \times n})$ is the force density matrix and $\mathbf{x}, \mathbf{y}, \mathbf{z}$ $(\in \Re^{n})$ are the nodal coordinate vectors. The symbol $[]^{\mathrm{T}}$ represents the transpose operation of a matrix or vector. The connectivity matrix $\mathbf{C}$ $(\in \Re^{m \times n})$ describes the connections between the n nodes of the tensegrity in the following way: if a general member j connects nodes i and k (with $i < k$), the ith and kth elements of the jth row of $\mathbf{C}$ are set to 1 and -1 respectively. Matrix $\mathbf{Q}$ $(\in \Re^{m \times m})$ is a diagonal square matrix that collects
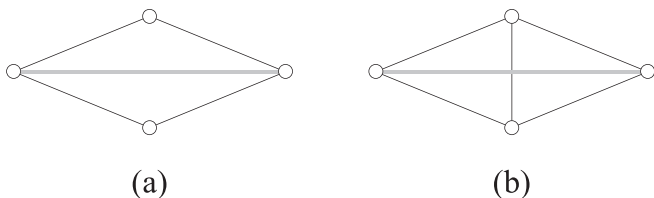

Fig. 1. Rhombic (a) and X-rhombic (b) elementary cells (black and grey lines correspond to cables and struts respectively).

the values of the force:length ratios q of each of the m members of the tensegrity. The force:length ratio q of each member of the family and the connectivity matrix $\mathbf{C}$ are the inputs of the form-finding methods based on FDM [9,11]. Matrix $\mathbf{D}$ can be directly formulated from the values of the force:length ratios of the members as shown in Eq.(2).

$$\mathbf{D}_{ij} = \begin{cases} \sum_{k \in \Gamma} q_k & for\ i = j \\ -q_k & if\ nodes\ i\ and\ j\ are\ connected\ by\ member\ k \\ 0 & otherwise \end{cases} \tag{2}$$

In Eq.(2) Γ is the set of members connected to the node i.

It can be proved that a tensegrity structure is non-degenerate in a d-dimensional space provided that the rank deficiency of its force density matrix $\mathbf{D}$ is at least $d + 1$ [15,20]. This non-degeneracy condition is achieved by imposing that the characteristic polynomial of $\mathbf{D}$ ($p(\lambda) = \lambda^n + a_{n-1} \lambda^{n-1} + \ldots + a_1 \lambda + a_0$) has $d + 1$ zero roots [20]. Given that, by construction of $\mathbf{D}$, the sum in each row or column always equals zero, then coefficient a_0 of the characteristic polynomial is 0. Therefore, a rank deficiency of matrix $\mathbf{D}$ of at least $d + 1$ (i.e. non-degeneracy condition) is achieved by solving the system of equations shown in Eq. (3).

$$\begin{aligned} a_3(q_1, \ldots, q_m) &= 0 \\ a_2(q_1, \ldots, q_m) &= 0 \\ a_1(q_1, \ldots, q_m) &= 0 \end{aligned} \tag{3}$$

In the form-finding method proposed by Hernández-Montes et al. [20], Eq.(3) was analytically solved for all the cases studied. It can be seen that the coefficients a_1, a_2 and a_3 of Eq. (3) depend on the different values of q considered for cables and struts. Hence, the complexity of the form-finding problem is directly related with the number of different values of q considered in the tensegrity. A more detailed description of the analytical form-finding procedure used in this work can be seen in [20,23].

The null space of $\mathbf{D}$, or ker($\mathbf{D}$), is the subspace of all vectors $\boldsymbol{v} \in \Re^n$ that satisfy $\mathbf{D}\boldsymbol{v} = 0$. The dimension of ker($\mathbf{D}$) coincides with the multiplicity of 0 as eigenvalue of $\mathbf{D}$ (which, due to the non-degeneracy condition, is at least $d + 1$).

In the case of a three-dimensional (3D) tensegrity ($d = 3$), the coordinate vectors $\times, \mathbf{y}$ and $\mathbf{z}$ are of the form:

$$\begin{aligned} \mathbf{x} &= \alpha_1 \mathbf{v_1} + \alpha_2 \mathbf{v_2} + \alpha_3 \mathbf{v_3} + \alpha_4 \mathbf{v_4} \\ \mathbf{y} &= \beta_1 \mathbf{v_1} + \beta_2 \mathbf{v_2} + \beta_3 \mathbf{v_3} + \beta_4 \mathbf{v_4} \\ \mathbf{z} &= \gamma_1 \mathbf{v_1} + \gamma_2 \mathbf{v_2} + \gamma_3 \mathbf{v_3} + \gamma_4 \mathbf{v_4} \end{aligned} \tag{4}$$

Being $\alpha_i, \beta_i,$ and γ_i constants upon whose value the shape and position of the final tensegrity depend.

Note that if the system of equations in Eq.(3) has more than $d + 1$ solutions with 0 as eigenvalue, then a larger number of eigenvectors $\boldsymbol{v_i}$ could be used to define the coordinate vectors. In this work, and without loss of generality, it is considered that $\mathbf{x} = \mathbf{v_1}$, $\mathbf{y} = \mathbf{v_2}$ and $\mathbf{z} = \mathbf{v_3}$ for all the tensegrities, while ignoring the remaining eigenvectors.

Regarding stability, a tensegrity is said stable if its tangent stiffness matrix $\mathbf{K}$ is positive semi-definite (note that the potential energy is minimum for the configuration for which the structure is stable [23,36,37]). The stability of tensegrity structures, as well as the complete definition of the matrix $\mathbf{K}$, has been discussed in detail in [23,36,37]. To study stability, the cross-sectional area A and the elastic modulus E of the members of the tensegrity (i.e., cables and struts) must be known. In [37], it is assumed that the magnitude of prestress in a member of a conventional tensegrity structure is 1% of EA. In this work, two cross-sectional areas of the members are considered (one for cables and one for bars) such that the maximum prestress in both cases equals 1% of the product EA ($E = 200.000$ MPa), as in [23,37].

Super-stability is a most robust criterion. According to [35–37], a tensegrity is considered as super-stable if it is stable regardless of the material properties and prestress levels. The super-stability conditions are the following: *i)* the rank deficiency of the force density matrix $\mathbf{D}$ (Eq.(2)) is $d + 1$, *ii)* matrix $\mathbf{D}$ is positive semi-definite, and *iii)* the rank of

the geometry matrix **G** is $d(d+1)/2$. An in-depth explanation on the superstability and on the geometry matrix **G** can be seen in [23,36,37].

3. The Octahedron and the x-octahedron families of tensegrities

The Octahedron [23,33] and the X-Octahedron [32] are examples of tensegrity families shown in the literature. These families are made up of tensegrities that share a common topology or connectivity pattern. Each member has a position into the family, denoted by p, with the first member corresponding to $p = 1$, the second to $p = 2$ and so on. The number of nodes, cables and struts in each member increase as its position in the family gets higher. The nodes in the full forms of tensegrity structures have different positions in the equilibrium configuration, while in the folded forms, some nodes share the same position in space [20]. With the exception of the first member ($p = 1$), to obtain the full form of each member in the family, the previous member is expanded by duplicating each node, cable, and strut. So, in a tensegrity family, each member (full form) contains all the previous members of the family as folded forms [20,23,31–34].

The Octahedron family [23,33] and the first three members of the X-Octahedron family [32] are examples of tensegrities based on topology available in the literature. In [33] the topology of the Octahedron family was presented. An endless number of tensegrities belonging to the Octahedron family can be obtained using an identical topological rule, which is very easy to implement. This topology was defined based on the expansion of a member to the subsequent one. As can be seen in [33], the growth of a tensegrity from one member to the next involves duplicating the number of rhombic cells and using a witty node numbering.

Each elementary cell in the Octahedron family is formed by four nodes connected through four cables and one strut (see the rhombic cell in Fig. 1.a). In the rhombic cell of Fig. 1.a two types of nodes can be defined: principal (not connected by the strut) and secondary nodes (connected by the strut). The general connectivity pattern presented in [33] for the definition of the member p of the Octahedron family is rewritten as follows (see Fig. 2.b, which corresponds to $p = 3$):

(i) Draw a $3 \times 2^{(p-2)}$ matrix of paired rhombic cells, as shown in Fig. 2.b, with each cell of the pair overlapping the other.
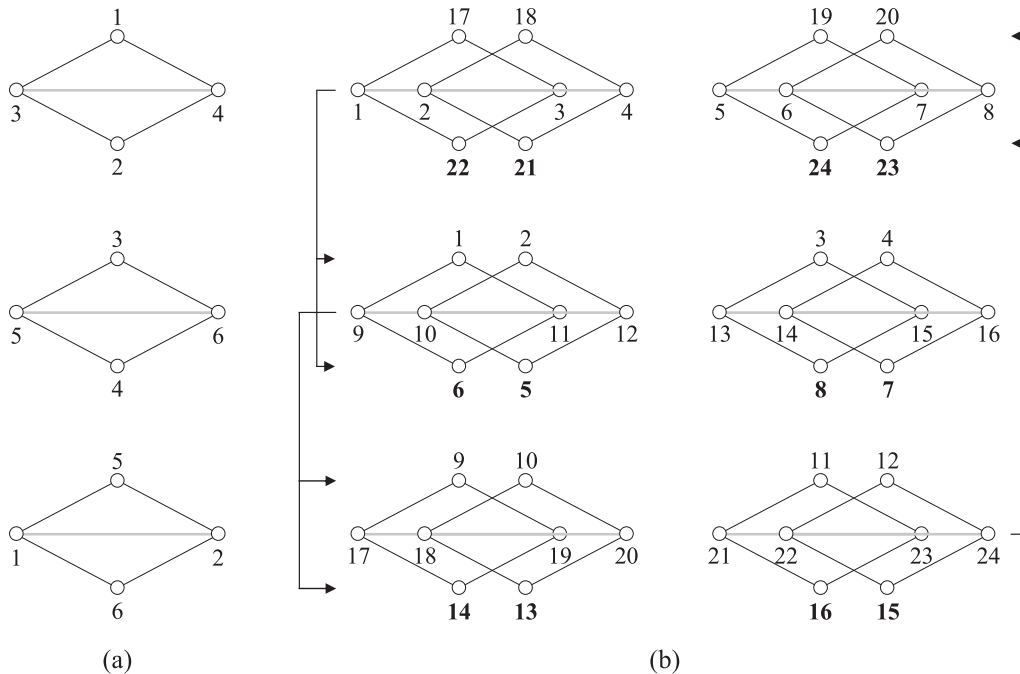
(ii) Number the secondary nodes in consecutive order from the first row to the third one.

(iii) Number the principal nodes of a row as the secondary ones of the previous row (see lateral arrows in Fig. 2.b) in a consecutive order from left to right and from top to bottom.

(iv) Swap the number of the nodes below the struts of each pair of rhombic cells (see the bold numbers in Fig. 2.b).

Because the rules above are not valid for the octahedron, its connectivity graph is depicted in Fig. 2.a. Note that the topology of the Octahedron family shown in Fig. 2.b is exactly the same than that presented in [33].

If an extra cable is added in the rhombic cells of Fig. 2, a X-diamond or X-rhombic elementary cell is obtained (see Fig. 1.b). This cell is the elementary cell of the X-Octahedron family introduced in [32], whose connectivity pattern is the same than that of the Octahedron family, as shown in Fig. 3.b. So, the members of the X-Octahedron family are obtained by replacing the rhombic cells of the members of the Octahedron family with X-rhombic cells while keeping the connectivity pattern
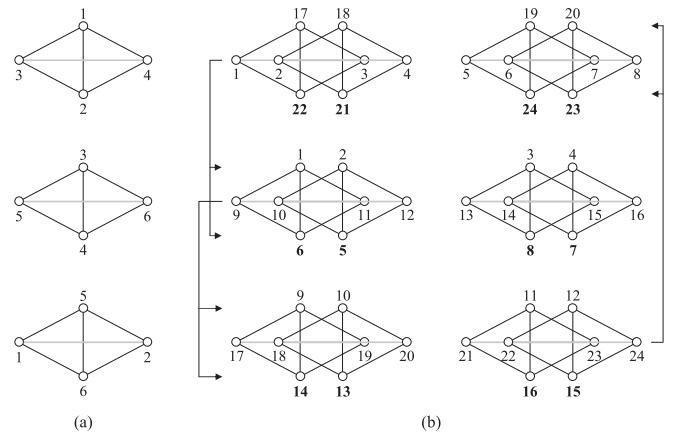

Fig. 3. Connection graph of the X-octahedron ($p = 1$) (a) and general connectivity pattern of the X-Octahedron family (case of $p = 3$) (b).

Fig. 2. Connection graph of the octahedron ($p = 1$) (a) and general connectivity pattern of the Octahedron family (case of $p = 3$) (b).

unchanged. This design method based on cell substitution has been used in [22,31,38]. As in the case of the Octahedron family, the topology of the X-Octahedron family is not valid for its first member (X-octahedron, $p = 1$), whose connection graph is the one depicted in Fig. 3.a.

Once the elementary cells of each member of the Octahedron or the X-Octahedron family have been defined based on topology (see Figs. 2 and 3), the corresponding matrix **C** can be easily constructed.

As can be observed in Figs. 2 and 3, the connectivity pattern is composed of nodes connected by links or lines. Hence, the connectivity between the nodes of the members of the tensegrity families can be treated as a graph. In fact, structures with regular patterns, like the ones considered in this study, can be interpreted as the result of Boolean operations (graph products) involving multiple simple graphs or subgraphs. Indeed, the principles of graph theory have proved to be very useful for describing pin-jointed structures such as in [39,40].

The analytical form-finding method shown in Section 2 is used here to compute the force:length ratios that lead to equilibrium configurations of the tensegrities fulfilling the non-degeneracy condition.

The computational complexity of the analytical form-finding method increases as the number of different values of force:length ratios considered also increases. In this study, without loss of generality, just two values of q are going to be considered: q_c for cables and q_b for struts/bars.

Once the characteristic polynomial $p(\lambda)$ of the resulting matrix **D** is computed, the resolution of the system of equations shown in Eq.(3) $\{a_1(q_c, q_b) = 0, a_2(q_c, q_b) = 0, a_3(q_c, q_b) = 0\}$ leads to the values of force:length ratios for which configurations of equilibrium of the 3D tensegrity structure exist. The solution of the previous system of equations which leads to full forms of tensegrities for the $p = 1$, $p = 2$, $p = 3$ and $p = 4$ members of the Octahedron family are $q_b/q_c = -2, -3/2, -4/3$ and $-5/4$, respectively [33]. It is worth noting that, if the same element grouping and connectivity pattern are considered, both the analytical method proposed in [20] and the numerical methods, such as the one presented in [19], should lead to the same solutions.

The solutions of the form-finding problem of the Octahedron family (in terms of the ratio q_b/q_c) follow a certain mathematical sequence that depends on the position of the tensegrity in the family (p). The sequence of values of q_b/q_c solutions for Eq.(3) for tensegrities of the Octahedron family [30] is shown in Eq.(5) (proposed in [33]). On the other hand, in [32] only the first three members of the X-Octahedron family are presented. It can be verified that the solutions of Eq.(3) corresponding to the full forms for the $p = 1$, $p = 2$ and $p = 3$ members of the X-Octahedron family are $q_b/q_c = -3, -5/3, -7/5$, respectively [32]. Operating in the same way as in the case of the Octahedron family, the sequence of values of q_b/q_c solutions for Eq.(3) corresponding to the X-Octahedron family is the one indicated in Eq.(6). Consequently, an endless number of

tensegrity structures that belong to the X-Octahedron family can be obtained (see the examples shown in Fig. 4). Moreover, the values of ratio q_b/q_c obtained from Eqs.(5) or (6) for the p-th member of each family lead to a super-stable full-form tensegrity.

$$\frac{q_b}{q_c} = -\frac{p+1}{p} \tag{5}$$

$$\frac{q_b}{q_c} = -\frac{2p+1}{2p-1} \tag{6}$$

Since the ratio q_b/q_c can be determined using Eqs.(5) and (6), for the Octahedron and X-Octahedron families, respectively, the form-finding problem is reduced to the calculation of the eigenvectors of matrix **D** (Eq.(2)), and the resolution of the system of equations in Eq.(3) is no longer necessary.

The mathematical sequences shown in Eqs.(5) and (6) are depicted in Fig. 5, where the super-stable equilibrium configurations of the full-forms of the members $p = 2$ and 3 have been represented.

Fig. 5 and Eqs.(5) and (6) show that both the Octahedron and the X-Octahedron families have an endless number of super-stable tensegrities.

4. Influence of the level of connectivity: disconnected, partially connected and full connected patterns in tensegrities of the Octahedron and X-Octahedron families

As seen in the previous section, in both the Octahedron and X-Octahedron families, each member comes from the expansion of the previous one from duplication of its elementary cells (and consequently, the number of nodes, cables, and struts is also doubled). Indeed, it might be said that each member is made up of two previous members connected between them following the connectivity pattern of the family. For example, the double-expanded octahedron (which has 12 rhombic cells) is made up by merging or connecting two expanded octahedrons (each of which has 6 rhombic cells).

In this work, the term "twin" refers to the two tensegrities from the same position of the family that are connected to each other in order to make up the subsequent member. Thus, the p member of the family is the result of connecting two twin (p-1) members.

The tensegrity members of both the Octahedron and X-Octahedron families studied in this work have elementary cells grouped in three rows, as shown in Figs. 2 and 3. These three rows are connected to each other, resulting in three levels of connectivity (as indicated by the arrows in Fig. 2.b and 3.b). Up to this point, the tensegrities of both families have been built based on these three levels of connectivity. However, as shown below, different tensegrity structures of both
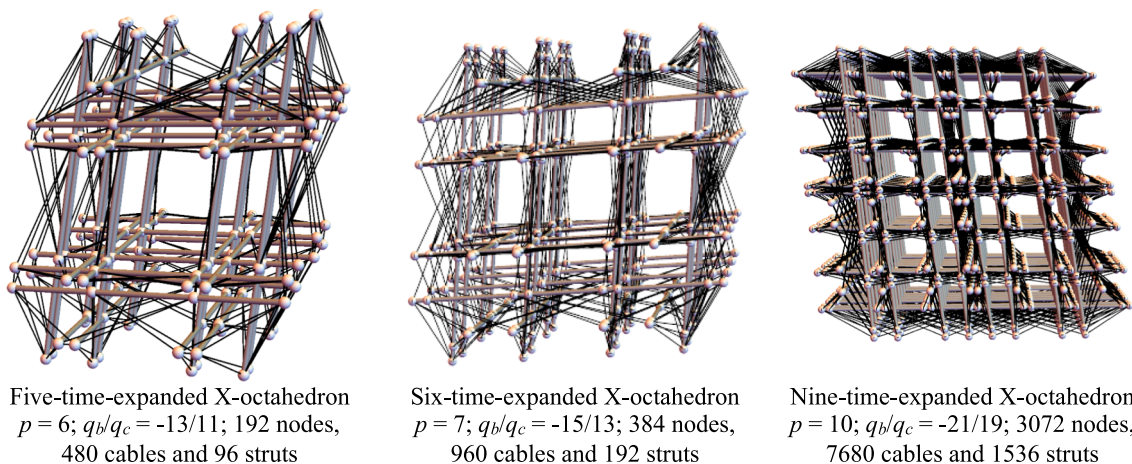

Five-time-expanded X-octahedron
$p = 6$; $q_b/q_c = -13/11$; 192 nodes, 480 cables and 96 struts

Six-time-expanded X-octahedron
$p = 7$; $q_b/q_c = -15/13$; 384 nodes, 960 cables and 192 struts

Nine-time-expanded X-octahedron
$p = 10$; $q_b/q_c = -21/19$; 3072 nodes, 7680 cables and 1536 struts

Fig. 4. Five-time-expanded X-octahedron (a), six-time-expanded X-octahedron (b), and nine-time-expanded X-octahedron (c).
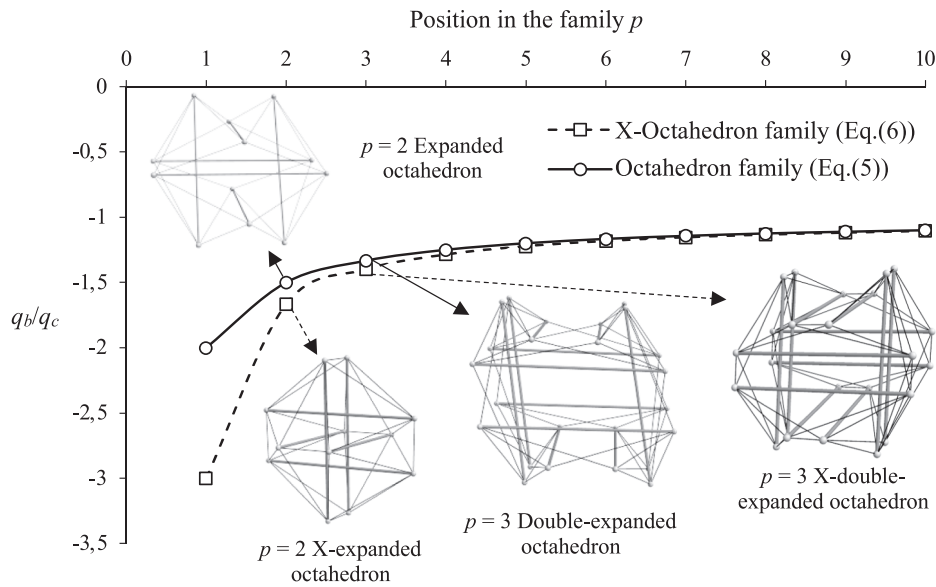
Fig. 5. Sequence of solutions of q_b/q_c of the Octahedron and X-Octahedron families shown in Eqs.(5) and (6) respectively.

families can be obtained by modifying the connection level between the rows of the cells. In this work, the level of connectivity is indicated as a subscript in the position of the family. Hence, the tensegrity of the Octahedron family $p = 3_2$ corresponds to a double-expanded octahedron made up by two expanded octahedrons connected at two levels. The full connection (three levels of connectivity) cases do not have any subscript.

For the sake of simplicity, only two values of q are going to be considered in all the tensegrities shown in this section: q_c for cables and q_b for struts. Furthermore, the stability analysis is conducted considering the material properties described in Section 2, and $q_c = 1$ (whose force and length units are in accordance with the units of the elastic modulus and of the cross-sectional area) is adopted.

4.1. Disconnected or zero level of connectivity in the Octahedron and X-Octahedron connectivity patterns

Fig. 6 shows two twin expanded octahedrons ($p = 2$), A and B, with nodes connected according to the connectivity pattern of the Octahedron family indicated in Fig. 2.b. As can be seen in Fig. 6, no connection exists between the cells of the two twins, indicating a zero connectivity level ($p = 3_0$). Fig. 6 can also be applied to the X-Octahedron family by adding a cable between the principal nodes of each cell (see Fig. 3).

It can be proven that the equilibrium configuration of the two twin tensegrities shown in Fig. 6, A and B, can be obtained from Eq.(3) once the force density matrix **D** corresponding to the two twin tensegrities is built. Table 1 summarizes the results of the form-finding problem for a zero level of connectivity for four different cases: two twins expanded and double-expanded octahedrons, and two twins expanded and double-expanded X-Octahedrons.

As can be seen in Table 1, some stable equilibrium configurations are obtained, all of them corresponding to the lowest value of q_b/q_c in each case. It is worth noting that the ratios q_b/q_c obtained for both the expanded octahedron and the X-expanded octahedron follow the sequences given by Eqs.(5) and (6), respectively.

4.2. One and two levels of connectivity in the Octahedron and X-Octahedron connectivity patterns

Let us now connect the two twin tensegrities A and B of Fig. 6 at one and two levels of connectivity (see dotted lines in Fig. 7 and Fig. 8, respectively). As can be seen in Fig. 7 (corresponding to one level of connectivity), the principal nodes of row 2 are numbered as the
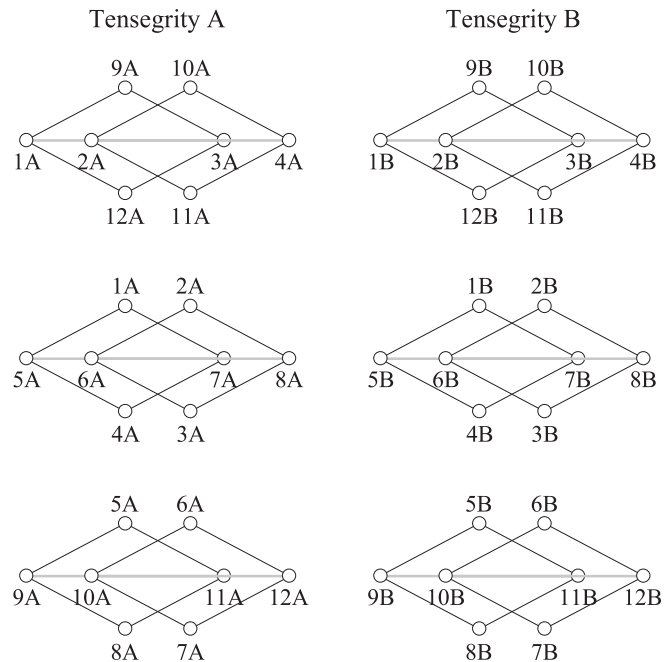

Fig. 6. Two twin expanded octahedrons (A and B) with zero connectivity level $p = 3_0$ (i.e. there is no connection between them).

Table 1
Solutions of the form-finding problem of twin tensegrities belonging to both the Octahedron and the X-Octahedron families with zero level of connectivity.

Tensegrity	Solutions of Eq. (3)	Stability
Double expanded octahedron $p = 3_0$	$q_b/q_c = -2$	Unstable
	$q_b/q_c = -3/2$	Stable
Triple expanded octahedron $p = 4_0$	$q_b/q_c = -2$	Unstable
	$q_b/q_c = -3/2$	Unstable
	$q_b/q_c = -4/3$	Stable
X-double expanded octahedron $p = 3_0$	$q_b/q_c = -3$	Unstable
	$q_b/q_c = -5/3$	Stable
X-triple expanded octahedron $p = 4_0$	$q_b/q_c = -3$	Unstable
	$q_b/q_c = -5/3$	Unstable
	$q_b/q_c = -7/5$	Stable

Tensegrity A

9A 10A

1A 2A 3A 4A

12A 11A

1A 2A 3A 4A

5A 6A 7A 8A

2B 1B 4B 3B

5A 6A

9A 10A 11A 12A

8A 7A

Tensegrity B

9B 10B

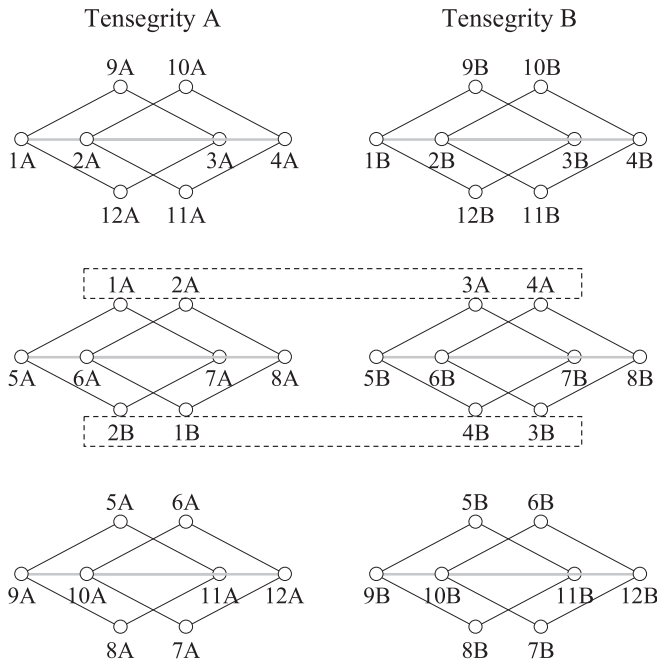1B 2B 3B 4B

12B 11B

3A 4A

5B 6B 7B 8B

4B 3B

5B 6B

9B 10B 11B 12B

8B 7B

Fig. 7. Two twin expanded octahedrons (A and B) connected at one connectivity level (which corresponds with $p = 3_1$).

Tensegrity A
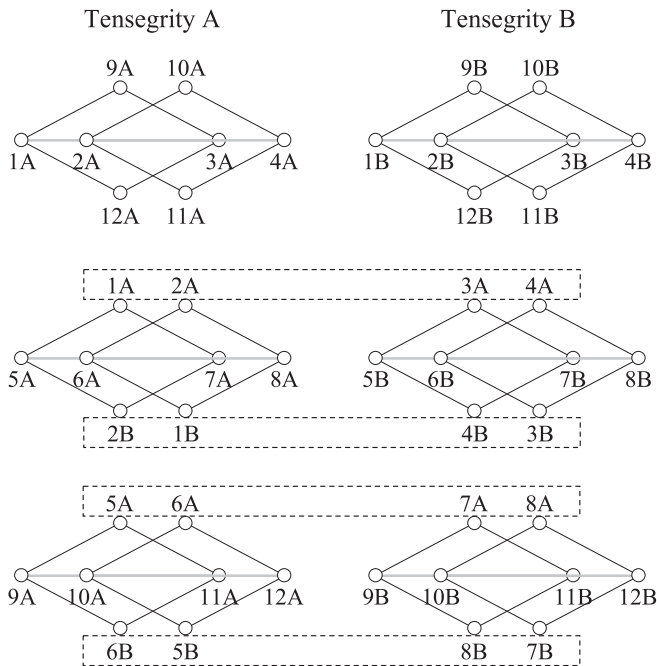
9A 10A

1A 2A 3A 4A

12A 11A

1A 2A 3A 4A

5A 6A 7A 8A

2B 1B 4B 3B

5A 6A 7A 8A

9A 10A 11A 12A

6B 5B 8B 7B

Tensegrity B

9B 10B

1B 2B 3B 4B

12B 11B

3A 4A

5B 6B 7B 8B

4B 3B

7A 8A

9B 10B 11B 12B

8B 7B

Fig. 8. Two twin expanded octahedrons (A and B) connected at two connectivity levels (which corresponds with $p = 3_2$).

secondary ones of row 1 following the rule presented in Section 3 and Fig. 2.b. On the other hand, in the case of two levels of connectivity, the connectivity pattern is extended to two rows, so the principal nodes of rows 2 and 3 are numbered as the secondary ones of rows 1 and 2, respectively (see Fig. 8).

Given that the connectivity pattern of the X-Octahedron family is the same than that of the Octahedron family, Figs. 7 and 8 are also applicable to the X-Octahedron family just adding a cable between the principal nodes of each cell. Table 2 summarizes the results of the form-finding problem for one level of connectivity (as shown in Fig. 7) for the

Table 2
Solutions of the form-finding problem of the double-expanded octahedron ($p = 3_1$) and the triple-expanded octahedron ($p = 4_1$) considering one level of connectivity. Red and blue struts correspond to each twin tensegrity and green struts correspond to two overlapped struts (for the interpretation of the references to color, the reader is referred to the online version of this article).

Tensegrity	Solutions of Eq. (3)	Stability	Equilibrium configuration
Double-expanded octahedron ($p = 3_1$)	$q_b/q_c = -2$ $q_b/q_c = -3/2$	Unstable Unstable	
Triple-expanded octahedron ($p = 4_1$)	$q_b/q_c = -2$ $q_b/q_c = -3/2$ $q_b/q_c = -4/3$	Unstable Unstable Stable	

double-expanded octahedron ($p = 3_1$, made up by two twin expanded octahedrons) and for the triple-expanded octahedron ($p = 4_1$, made up by two twin double-expanded octahedrons). The same cases are considered for the X-Octahedron family, and the results are presented in Table 3. Values of the ratio q_b/q_c in Tables 2 and 3 have been obtained by solving the system of equations shown in Eq.(3). It can be observed that the ratios q_b/q_c shown in Tables 2 and 3 follow the mathematical sequences given by Eqs.(5) and (6) for each family of tensegrities and for the value of p of each twin tensegrity connected.

The equilibrium configurations corresponding to the lowest value of

Table 3
Solutions of the form-finding problem of the X-double-expanded octahedron ($p = 3_2$) and the X-triple-expanded octahedron ($p = 4_2$) considering one level of connectivity. Red and blue struts correspond to each twin tensegrity and green struts correspond to two overlapped struts (for the interpretation of the references to color, the reader is referred to the online version of this article).

Tensegrity	Solutions of Eq. (3)	Stability	Equilibrium configuration
X-double-expanded octahedron ($p = 3_2$)	$q_b/q_c = -3$ $q_b/q_c = -5/3$	Unstable Unstable	
X-triple-expanded octahedron ($p = 4_2$)	$q_b/q_c = -3$ $q_b/q_c = -5/3$ $q_b/q_c = -7/5$	Unstable Unstable Stable	

the ratio q_b/q_c (i.e., the full form [20]) are depicted in the fourth column of Tables 2 and 3. In these configurations, the struts of each of the two twin tensegrities connected have been drawn in different colors to allow the identification of each twin tensegrity.

Tables 2 and 3 show that, when considering one level of connectivity, a significant number of tensegrities of both the Octahedron and the X-Octahedron families are unstable for the materials properties and the level of prestress considered in this study.

Table 2 shows that for the triple-expanded octahedron $p = 4_1$ (made up by two twin double-expanded octahedrons at one level of connectivity), the solution $q_b/q_c = -4/3$ leads to a stable equilibrium configuration. On the other hand, the triple-expanded octahedron $p = 4$ defined in [33] and built using three levels of connectivity or full connection (see the connectivity pattern shown in Fig. 3.b), has a super-stable equilibrium configuration for the solution $q_b/q_c = -5/4$. However, in this configuration some struts line up on top of each other [33], making it impossible to construct. This is not the case for the $p = 4_1$ tensegrity, in which no bar is overlapped with another one. Hence, the reduction of the level of connectivity from three to one has a negative effect on the stability of the triple-expanded octahedron but improves its constructability given that the struts are not lined up. The above represents an important step towards the construction of the members of the Octahedron family.

In Table 3, it can be seen that the full form of the X-triple-expanded octahedron $p = 4_1$ has a stable equilibrium configuration for $q_b/q_c = -7/5$. Moreover, in this equilibrium configuration, neither the struts nor the cables are lined up, which is an important advantage for construction purposes. This is in contrast to the X-triple-expanded octahedron connected at three levels of connectivity ($p = 4$), where some struts and cables are lined up one on top of each other.

The results for the Octahedron and X-Octahedron families with two levels of connectivity (as shown in Fig. 8) are summarized in Tables 4 and 5, respectively. In both tables, the results corresponding to the double-expanded and triple-expanded tensegrities are summarized.

Tables 4 and 5 show that the solutions obtained for the two levels of connectivity also follow the mathematical sequences given in Eqs.(5) and (6) for each family of tensegrities. However, in this case, the solutions correspond to a tensegrity one level above each twin tensegrity,

Table 4

Solutions of the form-finding problem of the double-expanded octahedron ($p = 3_2$) and the triple-expanded octahedron ($p = 4_2$) considering two levels of connectivity. Red and blue struts correspond to each twin (for the interpretation of the references to color, the reader is referred to the online version of this article).
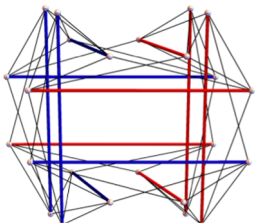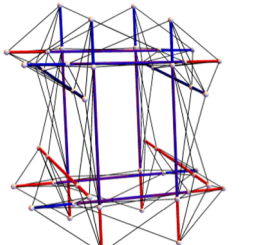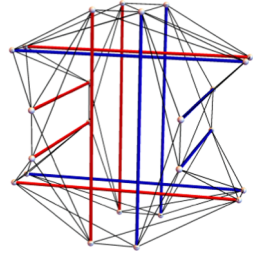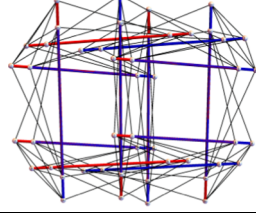
Tensegrity	Solutions of Eq. (3)	Stability	Equilibrium configuration
Double-expanded octahedron ($p = 3_2$)	$q_b/q_c = -2$ $q_b/q_c = -3/2$ $q_b/q_c = -4/3$	Unstable Stable Super-stable	
Triple-expanded octahedron ($p = 4_2$)	$q_b/q_c = -2$ $q_b/q_c = -3/2$ $q_b/q_c = -4/3$ $q_b/q_c = -5/4$	Unstable Unstable Stable Super-stable	

Table 5

Solutions of the form-finding problem of the X-double-expanded octahedron ($p = 3_2$) and the X-triple-expanded octahedron ($p = 4_2$) considering two levels of connectivity. Red and blue struts correspond to each twin (for the interpretation of the references to color, the reader is referred to the online version of this article).

Tensegrity	Solutions of Eq. (3)	Stability	Equilibrium configuration
Double-expanded X-octahedron ($p = 3_2$)	$q_b/q_c = -3$ $q_b/q_c = -5/3$ $q_b/q_c = -7/5$	Unstable Stable Super-stable	
Triple-expanded X-octahedron ($p = 4_2$)	$q_b/q_c = -3$ $q_b/q_c = -5/3$ $q_b/q_c = -7/5$ $q_b/q_c = -9/7$	Unstable Stable Stable Super-stable	

obtaining the same solutions as those for the cases of three levels of connectivity (i.e., full connection pattern, see Fig. 2.b and 3.b). In other words, an additional solution is obtained compared to the case of one level of connectivity and the same solutions are obtained compared to the full connectivity case.

As with previous tables, the equilibrium configurations shown in Tables 4 and 5 correspond to the lowest value of the ratio q_b/q_c (which corresponds to the full form configuration). A comparison of Tables 2 and 3 with Tables 4 and 5 shows that increasing the level of connectivity results in an improvement of the stability conditions of the tensegrities. Furthermore, Tables 4 and 5 show that, with two levels of connectivity, super-stable configurations are achieved for all the full form of the tensegrities studied.

As stated in Section 2, the coordinate vectors for all the equilibrium configurations of the tensegrities in Tables 4 and 5 has been adopted as $\mathbf{x} = \mathbf{v_1}$, $\mathbf{y} = \mathbf{v_2}$ and $\mathbf{z} = \mathbf{v_3}$, with $\mathbf{v_4}$ and any other possible eigenvectors corresponding to the 0 eigenvalue has been ignored. However, it has been observed that the choice of the coordinate vectors can directly impact the stability of certain tensegrities. For example, the triple-expanded octahedron $p = 4_2$ with $q_b/q_c = -3/2$ shown in Table 4 is unstable when $\mathbf{x} = \mathbf{v_1}$, $\mathbf{y} = \mathbf{v_2}$ and $\mathbf{z} = \mathbf{v_3}$, but becomes stable if the coordinate vectors are defined as: $\mathbf{x} = \mathbf{v_4}$, $\mathbf{y} = \mathbf{v_2}$ and $\mathbf{z} = \mathbf{v_3}$. Similar cases have been observed for other tensegrities, which can be either stable or unstable depending on the choice of coordinate vectors. It is worth noting that in the tensegrities studied, the selection of coordinate vectors has not affected super-stability.

4.3. Three levels of connectivity (full connection pattern) in the Octahedron and X-Octahedron connectivity pattern

Finally, if two twin tensegrities are connected at three levels of connectivity according to patterns depicted in Figs. 2 and 3, depending on the family of tensegrities considered, the tensegrities already presented in [32,33] are obtained. To allow for comparison, results obtained from the connectivity patterns depicted in Figs. 2 and 3 are summarized in Tables 6 and 7, respectively.

Comparison of Table 4 with Table 6 and Table 5 with Table 7 shows that, for the cases studied, there is no difference between two and three levels of connectivity in the topological patterns and in the tensegrities

Table 6

Solutions of the form-finding problem of the double-expanded octahedron ($p = 3$) and the triple-expanded octahedron ($p = 4$) considering three levels of connectivity (full connection).
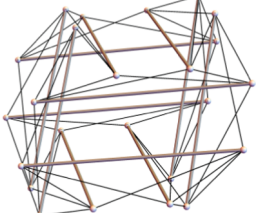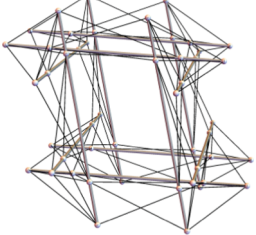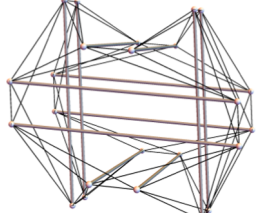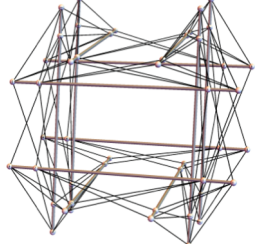
Tensegrity	Solutions of Eq. (3)	Stability	Equilibrium configuration
Double-expanded octahedron ($p = 3$)	$q_b/q_c = -2$ $q_b/q_c = -3/2$ $q_b/q_c = -4/3$	Unstable Stable Super-stable	
Triple-expanded octahedron ($p = 4$)	$q_b/q_c = -2$ $q_b/q_c = -3/2$ $q_b/q_c = -4/3$ $q_b/q_c = -5/4$	Unstable Stable Stable Super-stable	

Table 7

Solutions of the form-finding problem of the X-double-expanded octahedron ($p = 3$) and the X-triple-expanded octahedron ($p = 4$) considering three levels of connectivity (full connection).

Tensegrity	Solutions of Eq. (3)	Stability	Equilibrium configuration
Double-expanded X-octahedron ($p = 3$)	$q_b/q_c = -3$ $q_b/q_c = -5/3$ $q_b/q_c = -7/5$	Unstable Stable Super-stable	
Triple-expanded X-octahedron ($p = 4$)	$q_b/q_c = -3$ $q_b/q_c = -5/3$ $q_b/q_c = -7/5$ $q_b/q_c = -9/7$	Unstable Stable Stable Super-stable	

obtained. So, the q_b/q_c ratios that are solution of Eq.(3), and the equilibrium configurations of the tensegrities of the Octahedron and X-Octahedron families are the same for both two and three levels of connectivity. Furthermore, the stability does not even improve when the level of connectivity is increased from two to three.

To sum up, all the tensegrities studied in this work not only generate theoretical interest, but they are also of practical interest for engineering applications as a result of their cubic symmetry. For instance, they could be used as tensegrity metamaterials in impact protection systems, energy dissipation systems, and in adaptive load-bearing structures [41–43]. In addition, they could be used as modules for the design of structures such as pedestrian bridges [44,45].

5. Conclusions

The members of the Octahedron and of the X-Octahedron tensegrity families are composed by elementary cells (rhombic and X-rhombic cells, respectively). These cells are collected in three groups that are connected between them. Hence, the connectivity pattern of both families consists of three levels of connectivity.

In this work, the effect of the connectivity level on the members $p = 2$ and $p = 3$ of the Octahedron and X-Octahedron tensegrity families have been studied. Two tensegrities of the same position in the family (called "twins") have been connected between them considering different connectivity levels (zero, one and two). An analytical form-finding method has been used to compute the equilibrium configuration of the tensegrities. It has been verified that the ratio between the force:length ratios of struts and cables (q_b/q_c) leading to equilibrium configurations of the tensegrities follow the same mathematical sequence regardless of the level of connectivity, meaning that tensegrities of the same family can be obtained using partial connectivity patterns. Equilibrium configurations and stability conditions have been studied for the two families of tensegrities, as well as and for the cases of zero, full, one-level and two-levels of connectivity of two twin tensegrities. It has been proved that at least two levels of connectivity are required to obtain a ($p + 1$) tensegrity from two twin p tensegrities of both the Octahedron or X-Octahedron families.

On the other hand, the mathematical sequence that follows the ratio between the force:length ratio of struts and cables of the X-Octahedron family that leads to a super-stable equilibrium configuration is presented. In addition, it has been observed that the linear combination of the eigenvectors corresponding to the 0 eigenvalue, adopted as coordinate vectors, has a significant impact on the stability of the tensegrity. However, in the tensegrities studied here, the selection of the coordinate vectors has not affected super-stability, which happens for the lowest values of q_b/q_c. Further research is needed in this line. Results have interesting practical implications in the context of modular construction.

CRediT authorship contribution statement

Luisa Hernández: Investigation, Writing – original draft. **Manuel Alejandro Fernández-Ruiz:** Methodology, Investigation. **Luisa María Gil-Martín:** Conceptualization, Supervision, Writing – review & editing.

Declaration of Competing Interest

The authors declare that they have no known competing financial interests or personal relationships that could have appeared to influence the work reported in this paper.

Data availability

No data was used for the research described in the article.

References

[1] Feng Y, Yuan X, Samy A. Analysis of new wave-curved tensegrity dome. Eng Struct 2022;250:113408. https://doi.org/10.1016/j.engstruct.2021.113408.

[2] Feron J, Boucher L, Denoël V, Latteur P. Optimization of footbridges composed of prismatic tensegrity modules. J Bridg Eng 2019:24. https://doi.org/10.1061/(ASCE)BE.1943-5592.0001438.

[3] Yin X, Gao ZY, Zhang S, Zhang LY, Xu GK. Truncated regular octahedral tensegrity-based mechanical metamaterial with tunable and programmable Poisson's ratio. Int J Mech Sci 2020;167:105285. https://doi.org/10.1016/j.ijmecsci.2019.105285.

[4] Liu S, Li Q, Wang P, Guo F. Kinematic and static analysis of a novel tensegrity robot. Mech Mach Theory 2020;149:103788. https://doi.org/10.1016/j.mechmachtheory.2020.103788.

[5] Chen M, Goyal R, Majji M, Skelton RE. Design and analysis of a growable artificial gravity space habitat. Aerosp Sci Technol 2020;106:106147. https://doi.org/10.1016/j.ast.2020.106147.

[6] Scarr G. Biotensegrity: The structural basis of life. Handspring Publishing.; 2014.

[7] Gomez-Jauregui V, Otero C, Arias R, Manchado C. Innovative Families of Double-Layer Tensegrity Grids: Quastruts and Sixstruts. J Struct Eng 2013;139:1618–36. https://doi.org/10.1061/(asce)st.1943-541x.0000739.

[8] Gomez-Jauregui V, Quilligan M, Manchado C, Otero C. Design, fabrication and construction of a deployable double-layer tensegrity grid. Struct Eng Int 2018;28: 13–20. https://doi.org/10.1080/10168664.2018.1431379.

[9] Tibert AG, Pellegrino S. Review of Form-Finding Methods for Tensegrity Structures. Int J Sp Struct 2003;18:209–23. https://doi.org/10.1260/026635103322987940.

[10] Linkwitz K, Schek HJ. Einige Bemerkungen zur Berechnung von vorgespannten Seilnetzkonstruktionen. Ingenieur-Archiv 1971;40:145–58. https://doi.org/10.1007/BF00532146.

[11] Schek HJ. The force density method for form-finding and computation of general networks. Comput Methods Appl Mech Eng 1974;3:115–34. https://doi.org/10.1016/0045-7825(74)90045-0.

[12] Otter JRH. Computations for prestressed concrete reactor pressure vessels using dynamic relaxation. Nucl Struct Eng 1965;1:61–75. https://doi.org/10.1016/0369-5816(65)90097-9.

[13] Yuan S, Zhu W. Optimal self-stress determination of tensegrity structures. Eng Struct 2021;238:112003. https://doi.org/10.1016/j.engstruct.2021.112003.

[14] Tran HC, Lee J. Advanced form-finding of tensegrity structures. Comput Struct 2010;88:237–46. https://doi.org/10.1016/j.compstruc.2009.10.006.

[15] Zhang JY, Ohsaki M. Adaptive force density method for form-finding problem of tensegrity structures. Int J Solids Struct 2006;43:5658–73. https://doi.org/10.1016/j.ijsolstr.2005.10.011.

[16] Estrada GG, Bungartz H-J, Mohrdieck C. Numerical form-finding of tensegrity structures. Int J Solids Struct 2006;43:6855–68. https://doi.org/10.1016/j.ijsolstr.2006.02.012.

[17] Cai J, Feng J. Form-finding of tensegrity structures using an optimization method. Eng Struct 2015;104:126–32. https://doi.org/10.1016/j.engstruct.2015.09.028.

[18] Tran HC, Lee J. Form-finding of tensegrity structures using double singular value decomposition. Eng Comput 2011;29:71–86. https://doi.org/10.1007/s00366-011-0245-7.

[19] Koohestani K. A computational framework for the form-finding and design of tensegrity structures. Mech Res Commun 2013;54:41–9. https://doi.org/10.1016/j.mechrescom.2013.09.010.

[20] Hernández-Montes E, Fernández-Ruiz MA, Gil-Martín LM, Merino L, Jara P. Full and folded forms: a compact review of the formulation of tensegrity structures. Math Mech Solids 2018;23:944–9. https://doi.org/10.1177/1081286517697372.

[21] Vassart N, Motro R. Multiparameted form-finding method: application to tensegrity systems. Int J Sp Struct 1999;14:89–104. https://doi.org/10.1260/0266351991494768.

[22] Zhang LY, Li Y, Cao YP, Feng XQ. A unified solution for self-equilibrium and super-stability of rhombic truncated regular polyhedral tensegrities. Int J Solids Struct 2013;50:234–45. https://doi.org/10.1016/j.ijsolstr.2012.09.024.

[23] Fernández-Ruiz MA, Hernández-Montes E, Carbonell-Márquez JF, Gil-Martín LM. Octahedron family: The double-expanded octahedron tensegrity. Int J Solids Struct 2019;165:1–13. https://doi.org/10.1016/j.ijsolstr.2019.01.017.

[24] Zhang P, Fan W, Chen Y, Feng J, Sareh P. Structural symmetry recognition in planar structures using Convolutional Neural Networks. Eng Struct 2022;260: 114227. https://doi.org/10.1016/j.engstruct.2022.114227.

[25] Chen Y, Sun Q, Feng J. Improved Form-Finding of Tensegrity Structures Using Blocks of Symmetry-Adapted Force Density Matrix. J Struct Eng 2018;144: 04018174. https://doi.org/10.1061/(asce)st.1943-541x.0002172.

[26] Zhang JY, Guest SD, Ohsaki M. Symmetric prismatic tensegrity structures: Part I. Configuration and stability. Int J Solids Struct 2009;46:1–14. https://doi.org/10.1016/j.ijsolstr.2008.08.032.

[27] Li Y, Feng XQ, Cao YP, Gao H. Constructing tensegrity structures from one-bar elementary cells. Proc R Soc A Math Phys Eng Sci 2010;466:45–61. https://doi.org/10.1098/rspa.2009.0260.

[28] Zhang LY, Li Y, Cao YP, Feng XQ, Gao H. Self-equilibrium and super-stability of truncated regular polyhedral tensegrity structures: A unified analytical solution. Proc R Soc A Math Phys Eng Sci 2012;468:3323–47. https://doi.org/10.1098/rspa.2012.0260.

[29] Lee S, Lee J. A novel method for topology design of tensegrity structures. Compos Struct 2016;152:11–9. https://doi.org/10.1016/j.compstruct.2016.05.009.

[30] Kanno Y. Topology optimization of tensegrity structures under self-weight loads. J Oper Res Soc Japan 2012;55:125–45. https://doi.org/10.15807/jorsj.55.125.

[31] Fernández-Ruiz MA, Hernández-Montes E, Gil-Martín LM. The Z-octahedron family: A new tensegrity family. Eng Struct 2020;222:111151. https://doi.org/10.1016/j.engstruct.2020.111151.

[32] Fernández-Ruiz MA, Hernández-Montes E, Gil-Martín LM. The Octahedron family as a source of tensegrity families: The X-Octahedron family. Int J Solids Struct 2021;208–209:1–12. https://doi.org/10.1016/j.ijsolstr.2020.10.019.

[33] Fernández-Ruiz MA, Hernández-Montes E, Gil-Martín LM. Topological design of the Octahedron tensegrity family. Eng Struct 2022;259:114211. https://doi.org/10.1016/j.engstruct.2022.114211.

[34] Fernández-Ruíz MA, Hernández-Montes E, Gil-martín LM. From octagonal connection graphs belonging to the Z-Octahedron family to new tensegrity structures. Int J Solids Struct 2022;254–5. https://doi.org/10.1016/j.ijsolstr.2022.111901.

[35] Connelly R, Tensegrity structures.. Why are they stable? In: Thorpe MF, Duxbury PM, editors. Rigidity theory Appl. Kluwer Academic / Plenum Publishers; 1998. p. 47–54. https://doi.org/10.1007/0-306-47089-6_3.

[36] Zhang JY, Ohsaki M. Stability conditions for tensegrity structures. Int J Solids Struct 2007;44:3875–86. https://doi.org/10.1016/j.ijsolstr.2006.10.027.

[37] Zhang JY, Ohsaki M. Tensegrity Structures. Form, Stability, and Symmetry. Springer; 2015. doi:10.1007/978-4-431-54813-3.

[38] Feng XQ, Li Y, Cao YP, Yu SW, Gu YT. Design methods of rhombic tensegrity structures. Acta Mech Sin Xuebao 2010;26:559–65. https://doi.org/10.1007/s10409-010-0351-6.

[39] Chen Y, Feng J. Improved Symmetry Method for the Mobility of Regular Structures Using Graph Products. J Struct Eng 2016;142:04016051. https://doi.org/10.1061/(ASCE)ST.1943-541X.0001512.

[40] Kaveh A, Rahami H. An efficient method for decomposition of regular structures using graph products. Int J Numer Meth Eng 2004;61:1797–808. https://doi.org/10.1002/nme.1126.

[41] Ma Y, Zhang Q, Dobah Y, Scarpa F, Fraternali F, Skelton RE, et al. Meta-tensegrity: Design of a tensegrity prism with metal rubber. Compos Struct 2018;206:644–57. https://doi.org/10.1016/j.compstruct.2018.08.067.

[42] Bauer J, Kraus JA, Crook C, Rimoli JJ, Valdevit L. Tensegrity Metamaterials: Toward Failure-Resistant Engineering Systems through Delocalized Deformation. Adv Mater 2021;33:1–9. https://doi.org/10.1002/adma.202005647.

[43] Zhang LY, Yin X, Yang J, Li A, Xu GK. Multilevel structural defects-induced elastic wave tunability and localization of a tensegrity metamaterial. Compos Sci Technol 2021;207:108740. https://doi.org/10.1016/j.compscitech.2021.108740.

[44] Rhode-Barbarigos L, Hadj Ali NB, Motro R, Smith IFC. Designing tensegrity modules for pedestrian bridges. Eng Struct 2010;32:1158–67. https://doi.org/10.1016/j.engstruct.2009.12.042.

[45] de Albuquerque NB, Gaspar CMR, Seixas M, Santana MVB, Cardoso DCT. Design, fabrication and analysis of a bio-based tensegrity structure using non-destructive testing. Eng Struct 2022;265:114457. https://doi.org/10.1016/j.engstruct.2022.114457.